RESOURCE

nature medicine

Tumor grafts derived from women with breast cancer authentically reflect tumor pathology, growth, metastasis and disease outcomes

Yoko S DeRose[1], Guoying Wang[1], Yi-Chun Lin[1], Philip S Bernard[2,3], Saundra S Buys[4], Mark T W Ebbert[3], Rachel Factor[2], Cindy Matsen[5], Brett A Milash[6], Edward Nelson[5], Leigh Neumayer[5], R Lor Randall[7], Inge J Stijleman[2], Bryan E Welm[1,5] & Alana L Welm[1]

Development and preclinical testing of new cancer therapies is limited by the scarcity of *in vivo* models that authentically reproduce tumor growth and metastatic progression. We report new models for breast tumor growth and metastasis in the form of transplantable tumors derived directly from individuals undergoing treatment for breast cancer. These tumor grafts illustrate the diversity of human breast cancer and maintain essential features of the original tumors, including metastasis to specific sites. Co-engraftment of primary human mesenchymal stem cells maintains phenotypic stability of the grafts and increases tumor growth by promoting angiogenesis. We also report that tumor engraftment is a prognostic indicator of disease outcome for women with newly diagnosed breast cancer; orthotopic breast tumor grafting is a step toward individualized models for tumor growth, metastasis and prognosis. This bank of tumor grafts also serves as a publicly available resource for new models in which to study the biology of breast cancer.

Breast cancer is a serious healthcare problem and, despite improvements in early detection and treatment, kills more than 40,000 people per year in the United States alone. Even with marked progress toward understanding cancer biology, the translation of research findings into new therapies is still an enormous barrier to progress. Recent data suggests a 90% failure rate for new oncology drugs in the clinic[1].

Development of new therapies is limited by the scarcity of authentic *in vivo* models of human breast cancer with which researchers can examine the biology of tumors and how they metastasize and that can also be used for drug development. Construction of cancer cell lines and sublines as models for breast tumor progression[2], site-specific metastasis[3] and/or response to experimental therapeutics[4] have been very informative. However, breast cancer cell lines only partially recapitulate the genetic features[5,6] and metastatic potential of tumors in individuals with breast cancer, resulting in poor predictions of how drugs will perform in a clinical setting[1,7,8]. The divergence of cell lines from actual human tumors is probably due to selective pressures resulting from *in vitro* propagation, for example, growth on plastic and growth in the absence of a normal tissue microenvironment.

Engraftment of actual tumor tissues into immune-deficient mice (termed 'tumor grafts') provides improvement over implantation of cell lines in phenocopying human tumors, assaying tumor stem cell activity[9,10] and predicting drug responses in affected individuals[7,11–14]. Tumor-graft strategies for hormone-driven cancers such as breast or prostate cancer, however, have had limited success. In particular, the scarcity of models that show spontaneous, clinically relevant metastasis from breast tumors is concerning, given that the vast majority of deaths from breast cancer are caused by metastasis. Here we report the establishment of a unique bank of serially transplantable, orthotopic, subject-derived breast tumor grafts that retain crucial characteristics of the original tumor specimens, including metastasis.

RESULTS

Generation of tumor grafts for major types of breast cancer

We transplanted 49 fresh primary tumors or metastatic breast cancer cell samples, obtained immediately following surgery or fluid drainage from 42 different individuals, into cleared mammary fat pads of female nonobese diabetic severe combined immunodeficiency (NOD-SCID) mice. Tumors grew from 18 out of 49 samples (37%), and we successfully maintained 12 tumor lines from ten subjects through multiple rounds of serial transplantation (27% of the total samples). Five tumor grafts were estrogen receptor and progesterone receptor positive (ER^+PR^+), seven were ER and PR negative (ER^-PR^-) and five were positive for HER2 ($HER2^+$)

[1]Department of Oncological Sciences, Huntsman Cancer Institute, University of Utah, Salt Lake City, Utah, USA. [2]Department of Pathology, Huntsman Cancer Institute, University of Utah, Salt Lake City, Utah, USA. [3]The Associated Regional and University Pathologists Institute for Clinical and Experimental Pathology, Salt Lake City, Utah, USA. [4]Department of Internal Medicine, Medical Oncology Division, Huntsman Cancer Institute, University of Utah, Salt Lake City, Utah, USA. [5]Department of Surgery, Huntsman Cancer Institute, University of Utah, Salt Lake City, Utah, USA. [6]Bioinformatics Core Facility, Huntsman Cancer Institute, University of Utah Health Sciences Center, Salt Lake City, Utah, USA. [7]Department of Orthopaedic Surgery, Huntsman Cancer Institute, University of Utah, Salt Lake City, Utah, USA. Correspondence should be addressed to A.L.W. (alana.welm@hci.utah.edu).

Received 4 January; accepted 27 July; published online 23 October 2011; doi:10.1038/nm.2454

Table 1 Abbreviated data for each tumor and corresponding tumor graft line

	Subject information[a]						Xenograft information[a,b]				
ID	Source	Primary diagnosis[c]	ER status[d]	PR status[d]	HER2 status[d]	Clinical metastasis[e]	ER status[f]	PR status[f]	HER2 status[f]	Estrogen dependence[g]	Metastasis[h]
HCI-001	1° breast tumor	IDC	Neg	Neg	Neg	Lung	Neg	Neg	Neg	n/a	Lung, LN
HCI-002	1° breast tumor	IDC	Neg	Neg	Neg	LN	Neg	Neg	Neg	n/a	LN
HCI-003	1° breast tumor	IDC	Pos	Pos	Neg	LN	Pos	Pos	Neg	Yes	Lung, LN
HCI-004	1° breast tumor	IDC	Neg	Neg	Neg	Not detected	Neg	Neg	Neg	n/a	Not detected
HCI-005[i]	Pleural effusion	Mixed IDC and ILC	Pos	Pos	Pos	Lung, bone	Pos	Pos	Pos	Yes	Lung, LN, peritoneum
HCI-006[i]	Pleural effusion						Pos	Pos	Not tested	Not tested	Lung, LN, peritoneum
HCI-007[i]	Pleural effusion						Pos	Pos	Not tested	Not tested	Lung, LN, bone
HCI-008	Pleural effusion	IBC	Neg	Neg	Pos	Skin, lung	Neg	Neg	Pos	n/a	Lung, LN
HCI-009	Ascites	Poorly differentiated adenocarcinoma	Neg	Neg	Neg	LN, bone, pancreas, peritoneum	Neg	Neg	Neg	n/a	Lung, peritoneum LN
HCI-010	Pleural effusion	IDC	Neg	Neg	Neg	Lung	Neg	Borderline	Neg	n/a	Lung, LN
HCI-011	Pleural effusion	IDC	Pos	Pos	Neg	LN, pleura	Pos	Pos	Neg	No, but estrogen stimulated	Lung, LN
HCI-012	Pleural effusion	IDC	Neg	Neg	Pos	LN, pericardium	Neg	Neg	Pos	n/a	LN, thymus

[a]See **Supplementary Table 1** for additional information. [b]On the basis of at least three generations of transplantation. [c]IDC, infiltrating ductal carcinoma; ILC, infiltrating lobular carcinoma; IBC, inflammatory breast cancer. [d]On the basis of clinical diagnosis. [e]At last follow up. LN, lymph node. [f]See **Supplementary Figures 6–14**. [g]See **Supplementary Table 2**. n/a, not applicable. [h]At necropsy. [i]From the same individual, collected at different times. Pos, positive; Neg, negative.

(**Table 1** and **Supplementary Table 1**). Four of the grafts were from primary tumors, and eight were from metastatic effusions. Tumors that did not grow, or tumors that grew and then subsequently receded, comprised 20 primary tumors, 2 lymph node metastases, 2 bone metastases and 7 malignant effusions. Therefore, the source of the tumor (primary or metastasis) did not significantly predict successful engraftment (Fisher's exact test, $P = 0.09$) nor did ER or PR ($P = 0.99$) or HER2 status ($P = 0.25$).

To determine whether successful engraftment correlated with the amount of tumor in the fragments or the tumor-to-stroma ratios, we paraffin-embedded tumor fragments that had been preserved in parallel to transplantation (five fragments that successfully engrafted and five that did not). H&E staining of four to six fragments from each of the ten tumors revealed no clear differences in the tumor or stromal contribution to the fragments (**Supplementary Fig. 1** and data not shown).

Tumors that were ER negative (ER^-), progesterone receptor negative (PR^-) and HER2 negative ($HER2^-$), known as triple-negative breast cancers, usually grew the fastest (**Supplementary Fig. 2**); this is a phenomenon that has often been observed in the clinic[15]. Tumor growth rates for all subtypes tended to increase with serial passage, although these differences were not statistically significant (**Supplementary Figs. 3–5**). Because multiple research groups[16,17] have reported successful engraftment of primary tumors in more severely immunocompromised mice (the double mutant NOD-SCID *Il2rg*$^{-/-}$ (NSG) mice, which lack natural killer cells as well as mature lymphocytes[18]), we also tested the growth of several of our lines in NSG mice. Certain tumors (HCI-004 and HCI-008) grew faster in NSG mice, whereas others grew equally well in both strains (HCI-012; **Supplementary Table 1**).

Tumor grafts resemble the tumors from which they are derived

A clinical breast pathologist who was blinded to the identities of the samples evaluated all of the tumors. We stained each tumor with antibodies specific to wide-spectrum cytokeratins, E-cadherin, β-catenin and human vimentin to validate the epithelial nature of the tumors, and we stained for the clinical molecular markers ER, PR and HER2 (**Fig. 1** and **Supplementary Figs. 6–14**). We also analyzed the pathology of these samples (**Supplementary Table 1**). All tumor grafts retained the major characteristics of the original tumors, even following multiple passages in mice (we examined four to eight serially transplanted generations for each line).

The human-derived stroma was largely lost after engraftment, as assessed by loss of human vimentin protein in vimentin-negative tumors (**Supplementary Fig. 7**). This loss also resulted in enrichment of cytokeratin-positive cells (**Fig. 1** and **Supplementary Figs. 6–8**, **10** and **11**). To examine the presence of mouse stroma in the grafts, we performed staining for three cell types commonly found in tumors: leukocytes, fibroblasts and endothelial cells. Staining with antibodies specific to mouse CD45 revealed mouse leukocytic infiltration (**Supplementary Fig. 15**), whereas the grafts were negative for human-specific CD45 staining (see below). To discern human-derived compared to mouse-derived fibroblasts, we used two antibodies: an antibody specific to human vimentin and an antibody that recognizes both human and mouse vimentin. The dominant fibroblast population was derived from the mouse (**Supplementary Fig. 15**). We used the same strategy to determine the species of origin of the endothelial cells that formed the tumor vasculature using antibodies against CD31. We clearly detected mouse-derived endothelium but not human-derived endothelial cells (see below). Thus, tumor-associated stroma from the human samples was largely replaced by mouse-derived stroma in the tumor grafts.

The presence of ER in breast tumors is predictive of favorable response to hormone modulating therapies because of the dependence of tumor growth on estrogen. Although the majority (~70%) of newly diagnosed breast cancers are positive for ER, this tumor type is underrepresented in mouse models because of loss of ER expression or lack of estrogen dependence[19]. We tested whether the ER^+ tumor grafts retained estrogen dependence by growing them without estrogen supplementation with or without surgical ovariectomy. The ER^+ tumor grafts remained dependent on estrogen for tumor growth, were stimulated by estrogen or both, mimicking a key physiological characteristic of ER^+ breast tumors in humans (**Supplementary Table 2**).

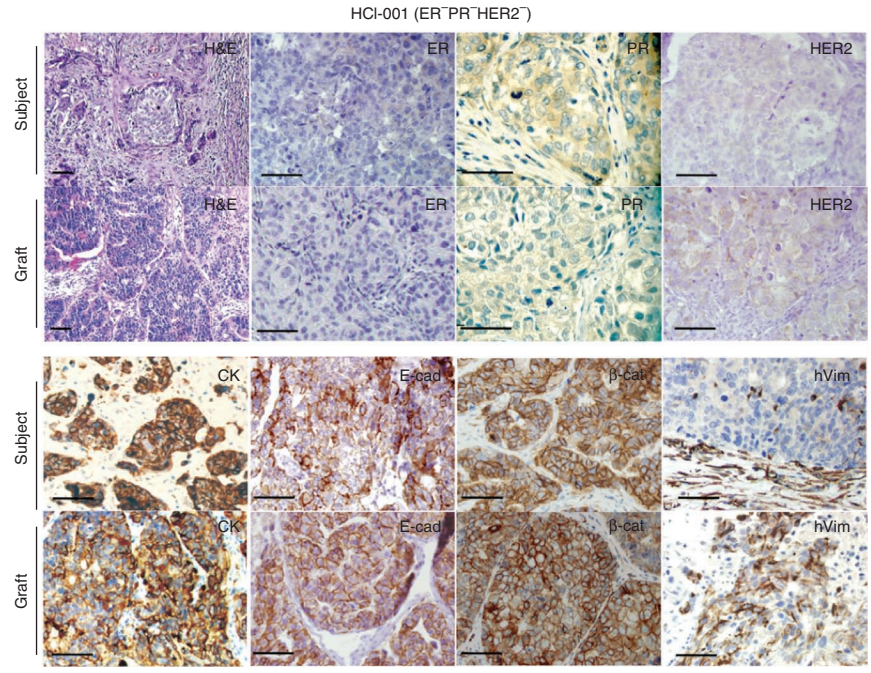

Figure 1 Tumor grafts resembled the original tumors from which they were derived. A representative ER⁻PR⁻HER2⁻ tumor graft (HCI-001) is shown in comparison to the original sample. The tumor identification number and the original clinical diagnosis for ER, PR and HER2 are shown at the top. Sections from the primary breast tumor of the subject and from representative tumor grafts from the same individual are shown. Shown are H&E stains, as well as antibody stains for ER, PR, HER2, cytokeratin (CK), E-cadherin (E-cad), β-catenin (β-cat) and human-specific vimentin (hVim). Positive antibody signals are shown in brown, and the hematoxylin counterstain is shown in blue. Some images are shown at higher magnification to visualize the nuclear staining. Scale bars, 100 μm.

Tumor grafts emulate metastasis seen in affected individuals

Human breast cancer cell lines are often poorly metastatic from the orthotopic site; however, the majority of the tumor grafts here were metastatic and generated patterns of metastasis similar to those seen in the original subjects. The most common site of metastasis in both the human subjects and the mice was the lymph nodes. In mice, the axillary nodes were most commonly involved (the inguinal nodes had been removed by mammary fat pad clearing during grafting), but we also found metastases in the thoracic and mesenteric nodes. We also detected spontaneous metastasis in the thymuses, lungs, bones and peritoneums of mice with tumor grafts (**Supplementary Table 1**). Metastases could be detected either grossly or by staining (**Fig. 2** and **Supplementary Figs. 16** and **17**).

The percentage of mice with metastasis varied between the tumor graft lines. We approximated the frequency of metastasis at the time of necropsy in three lines with different clinical profiles (HCI-011 ($ER^+PR^+HER2^-$), HCI-005 ($ER^+PR^+HER2^+$) and HCI-009 ($ER^-PR^-HER2^-$)) by examining three tumors from each of three different passages per line. Metastasis frequencies varied from 38% to 100% in these lines (**Supplementary Table 3** and **Supplementary Figs. 16** and **17**).

We also examined a small number of mice from these three lines as well as one subline of HCI-005 (HCI-007) in more detail for evidence of bone metastasis. We chose HCI-005, HCI-007 and HCI-009 because grafts in these lines were derived from individuals known to have developed bone metastasis. HCI-011 was derived from a person with ER^+ metastatic cancer that was refractory to hormone therapy. This type of tumor often metastasizes to bone, although at the time of this subject's death, she had not developed symptoms of bone metastasis. We detected ER^+, cytokeratin-positive bone micrometastasis in the HCI-007 line (**Supplementary Fig. 18**). Therefore, at least one tumor graft line is capable of spontaneous metastasis to bone; the HCI-007 line is derived from a woman that had bone metastasis (**Supplementary Table 1**). Future studies to determine whether bone metastasis occurs in other lines with or without resection of the primary tumor and/or with labeled tumor cells for increased sensitivity are underway.

Mesenchymal stem cells promote growth and stability of grafts

Growth of some tumor graft lines was limited by necrosis after initial engraftment, and we wondered whether the addition of human-derived stromal cells might overcome this problem. Cell line xenografts recruit bone marrow–derived mesenchymal stem cells (MSCs) to facilitate tumor growth and metastasis[20]. To determine whether MSCs facilitate tumor propagation in our models, we reimplanted established grafts together with primary human MSCs. We found that in all three of the lines we tested (two ER^- and one ER^+ line), MSCs increased tumor growth (**Fig. 3a**). We detected no statistically significant ($P = 0.38$) differences in tumor proliferation or apoptosis (**Supplementary Fig. 19**); however, grafts grown with MSCs had greater vascularity (**Fig. 3b**), which is consistent with the observation that tumors containing MSCs appeared bloodier than control tumors (**Fig. 3a**). Vessels were comprised of mouse endothelial cells

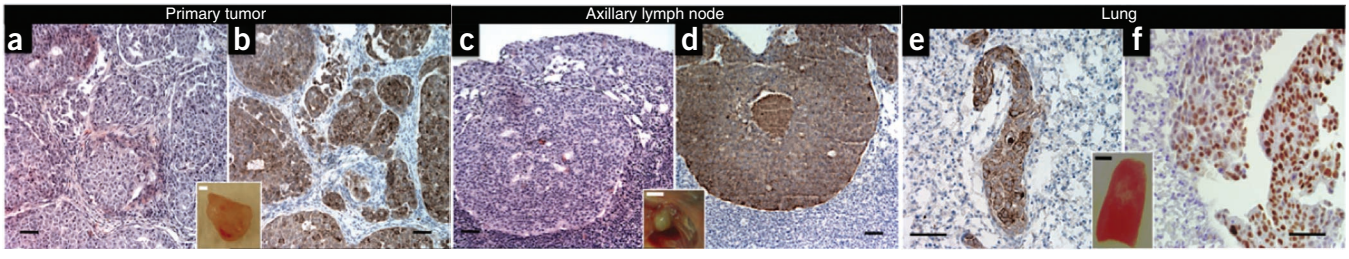

Figure 2 Tumor grafts spontaneously metastasized to clinically relevant sites. (**a**–**f**) Representative examples of a mammary tumor graft (primary tumor) and spontaneous metastases from HCI-011 cells as detected in sections of axillary lymph nodes and lungs of mice at necropsy. We identified metastases by routine histology (H&E; **a**,**c**) or by staining with antibodies specific to cytokeratin (**b**,**d**,**e**) or ER (**f**). Insets are representative pictures of each organ taken before fixing and embedding. Scale bars in the main panels, 100 μm, and inset scale bars, 3 mm.

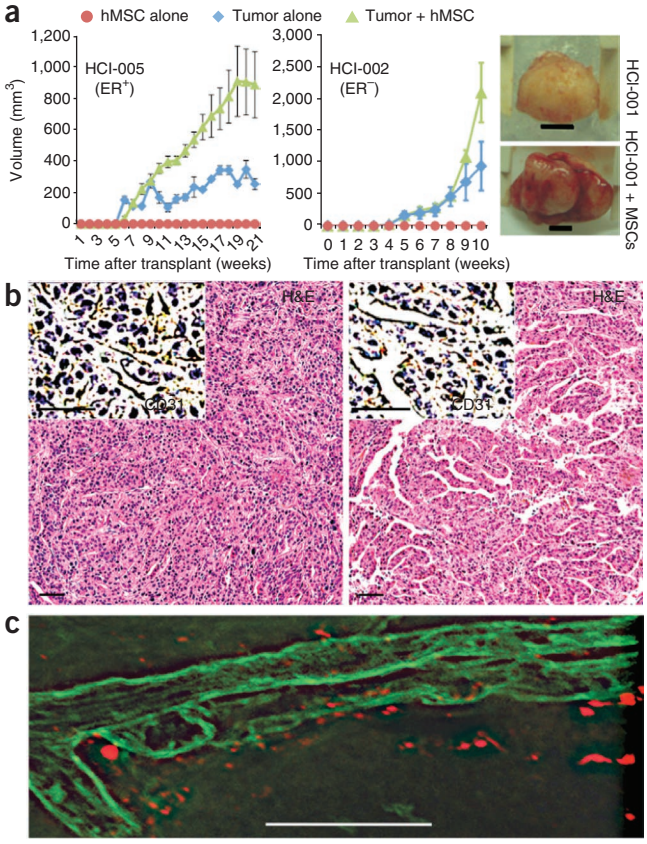

Figure 3 Co-engraftment of human mesenchymal stem cells (hMSCs) promotes vascularization and growth of tumor grafts. (**a**) Left and middle, growth rates for the cohorts of tumor grafts (derived from either the ER$^+$ tumor HCI-005 or the ER$^-$ tumor HCI-002) implanted either alone (blue diamonds) or with MSCs (green triangles). Mice injected with MSCs alone are indicated by red circles. Error bars, s.d. Right, photographs of representative tumors (derived from the ER$^-$ tumor HCI-001) grown with (bottom) or without (top) MSCs and isolated 59 d after transplantation. Tumors grown with MSCs were both bloodier and larger than those grown without MSCs. Scale bars, 5 mm. (**b**) H&E and antibody staining for CD31 (inset) identified elaborate vascular networks in tumor grafts in the presence of human MSCs (right) compared to the same tumor graft line growing in the absence of human MSCs (left). Scale bars, 100 μm. (**c**) Confocal microscopy on thick frozen tumor graft sections showed that blood vessels (identified by lectin staining, shown in green) are in close proximity to, but not comprised of, human MSCs (identified by dil label, shown in red). Scale bars, 100 μm.

(**Supplementary Fig. 20**). To determine whether MSCs also directly contribute to the vasculature, we labeled MSCs with fluorescent dye before injection. We found that the mouse-derived microvessels were not comprised of human MSCs; rather, MSCs were located adjacent to the vessels (**Fig. 3c**). These data suggest that MSCs enhanced tumor growth rates by supporting vascularization of tumors.

To determine whether addition of MSCs provided lasting effects on tumor growth, we carried out another round of transplantation of grafts that had been grown in the presence or absence of MSCs only in the previous generation. The resulting tumors showed no growth advantage because of the presence of MSCs in the first transplant (**Supplementary Fig. 21a**). These data indicate that, as previously noted[21], MSCs do not simply promote the selection of a preexisting, aggressive cell population within the tumor.

We also noted that the addition of MSCs correlated with strong ER positivity within ER$^+$ tumors. Although ER is clearly retained with serial passage of ER$^+$ tumor grafts without experimental exposure to MSCs, higher levels of ER staining were sustained after serial transplantation of tumors that had previously been grown with MSCs (**Supplementary Fig. 21b**,**c**). Together, these data suggest that MSCs have multiple, positive effects on human breast tumor grafts, including enhancement of vascularity and maintenance of ER protein expression. This is noteworthy, as loss of ER protein with tumor progression or serial transplantation is a common problem with models of ER$^+$ breast cancer[22].

Grafts retain the molecular features of tumors

Treatment decisions for individuals with breast cancer are currently determined by anatomic staging (tumor size, lymph node status and distant metastasis) and the presence or absence of molecular markers (ER, PR and HER2). However, the clinical behavior of tumors is better predicted by gene expression profiling[23–25]. A particularly successful strategy has been to stratify risk based on the 'intrinsic' molecular subtype of tumors[25–29]. Using an expanded set of these intrinsic genes[25], we assessed the molecular similarities between the original human tumors and their grafts. Unsupervised hierarchical clustering showed the overall relatedness of the tumors based on their gene expression profiles (**Fig. 4a**). All tumor and graft pairs clustered with each other (whether or not they were grown with human MSCs) and within a node containing other primary tumors of their subtype. We also classified the original tumors and grafts using the PAM50 supervised subtype predictor[25] and obtained similar results (**Supplementary Table 1**).

We performed a genome-wide single nucleotide polymorphism (SNP) microarray on all of the samples and used the resulting data to determine DNA copy number across the entire human genome. As with the gene expression data, the patterns of copy number variations found in the original tumors were typically maintained in tumor grafts (**Fig. 4b** and **Supplementary Figs. 22–31**). The most obvious changes were enhancement of existing aberrancies in grafts, presumably caused by the increased contribution of human tumor cells to the sample after grafting, as human stroma was replaced by mouse stroma (see above). The largest changes appeared in the ER$^+$ tumor grafts (for example, in HCI-003 and HCI-011 cells). We did not find changes common to all tumor grafts relative to their parent tumors, suggesting that copy number changes are not solely caused by growth in the mouse. Taken together, the gene expression and DNA copy number data provide evidence that tumor grafts maintain the prominent genomic and gene expression characteristics of the original tumors.

Prognostic value of orthotopic tumor grafts

Because successful engraftment of breast tumors did not correlate with the status of clinical markers (ER, PR or HER2) or with the tissue source (breast or a metastatic site), we postulated that the ability of a tumor to grow in mice might reflect a more aggressive phenotype that is independent of known clinical variables. Positive engraftment of tumor samples correlated with shorter survival across all subjects studied (**Fig. 5a**), indicating that the tumor grafts represent the most aggressive disease.

We also examined graft data and clinical outcome information from only individuals with newly diagnosed breast cancer who did not have detectable metastasis at the time of surgery. This comprised 24 individuals, whose median follow-up time was 28 months. Grafts were successfully maintained in four of those subjects (HCI-001, HCI-002, HCI-003 and HCI-004). There was no engraftment, or only transient

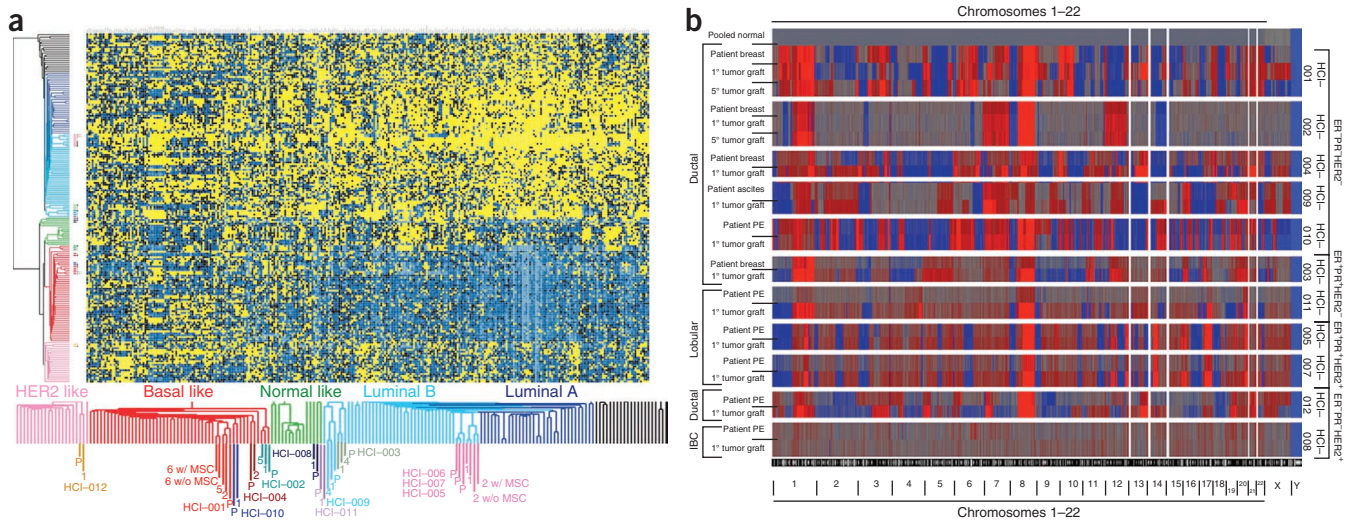

Figure 4 Gene expression and copy number variations found in the original tumors are well maintained in tumor grafts. (**a**) Hierarchical unsupervised clustering of microarray data from invasive breast cancers and tumor grafts using a set of 1,291 intrinsic genes. The dendrogram shows 'normal-like' breast tissue (light green) and the common cancer subtypes referred to as luminal A (dark blue), luminal B (light blue), HER2 enriched (pink) and basal like (red). Samples that did not clearly associate with any molecular subtype are shown in black. Each matched tumor or tumor graft is color coded (**Supplementary Table 1**) and is followed by a P or a number in the same color to distinguish the parent tumor from the tumor graft(s), respectively (the numbers correspond to the passage number in mice). The designation of with MSC (w/MSC) indicates array data from tumors coinjected with MSCs or the control tumors from the same experiments (indicated as w/o MSC). An enlarged view of the sample clusters is shown on the bottom for clarity. (**b**) Genome-wide SNP arrays are shown to illustrate DNA copy-number changes relative to normal DNA (isolated from blood donated by five disease-free females and then pooled; top row). Each tumor and the corresponding tumor graft (and, in some cases, tumor grafts that were serially passaged five times; 1° or 5°, respectively) are indicated on the left, along with the clinical type of breast cancer represented. Sample identities are shown on the right, along with the status of ER, PR and HER2. A copy number of two (defined as normal) is indicated in gray, a copy number greater than two (chromosomal gain or amplification) is shown in red, and a copy number of less than two (chromosomal loss or deletion) is shown in blue. The position of the copy number variants across the 22 autosomal chromosomes and 2 sex chromosomes is shown at the bottom. PE, pleural effusion; IBC, inflammatory breast cancer.

engraftment, of tumors from 20 subjects. We found that the ability of a tumor to successfully graft into the mouse mammary gland to be significantly correlated with reduced survival (**Fig. 5b**). Thus, the ability to generate stable orthotopic tumor grafts provided retrospective prognostic information about the course of the disease in the subjects we studied and, therefore, has potential to be used as a surrogate indicator of risk for disease progression. These data also provide evidence that tumor grafts are authentic models for the most aggressive tumor types, in addition to the fact that the grafts studied here were metastatic.

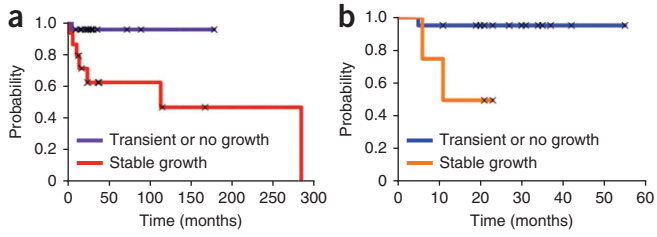

Figure 5 Successful growth of primary tumor specimens as tumor grafts significantly predicted shortened survival times. (**a**) A Kaplan-Meier survival analysis showing the probability of survival for all subjects. We stratified these subjects by whether their tumors did not grow or were not able to be maintained in mice (dark blue line) compared to those that did grow in mice (red line); $P = 0.02$ by log-rank statistics. (**b**) A Kaplan-Meier survival analysis showing probability of survival for individuals with newly diagnosed breast cancer whose primary tumors either did not grow or were not able to be maintained in mice (dark blue line) compared to those tumors that did grow in mice (orange line); $P = 0.01$ by log-rank statistics.

DISCUSSION

We established a bank of serially transplantable, orthotopic breast tumor grafts that retained critical characteristics of the original tumor specimens from living individuals with breast cancer (see also **Supplementary Fig. 32, Supplementary Results** and **Supplementary Discussion**). This work showed that (i) our current bank of grafts comprises all major clinical types of breast cancer, as well as multiple molecular subtypes; (ii) these grafts maintain key features of the original tumors, including histopathology, clinical markers, gene expression profiles, copy number variants and estrogen dependence and/or responsiveness; (iii) the addition of MSCs stimulates graft growth by increasing vascularization of the tumors and also contributes to maintenance of the expression of ER; (iv) the grafts spontaneously metastasize to many of the same organs that were affected in the subjects we studied; and (v) tumor engraftment is a prognostic factor for survival time, even in individuals with newly diagnosed breast cancer without known metastatic disease.

Although the mechanisms by which MSCs support tumor growth are beyond the scope of this report, it is plausible that they do so by enriching the microenvironment of the mouse mammary gland with human growth factors, proangiogenic factors and/or chemokines that favor tumor growth[30]. This effect may be similar to that previously described when mouse mammary fat pads were humanized with irradiated human fibroblasts[31]. Another possibility is that MSCs aid tumor growth by differentiating into specialized stromal cells in the tumor. MSCs do not appear to directly form blood vessels in tumors, however, despite the increased vascular density that we observed in their presence.

Co-injection of human MSCs did not markedly affect the number or size of the metastases in any of the lines we studied, possibly

because of the high frequency of metastasis already observed from grafts. Although MSCs consistently improved the growth of existing grafts, human MSCs also did not improve the 'take rate' of three different tumors that failed to engraft in NOD-SCID mice without human MSCs. The fact that MSCs only transiently promoted the growth of existing grafts is consistent with their effects on the host vasculature and also supports the notion of crosstalk between tumor cells, endothelial cells and MSCs. Crosstalk between tumor cells and MSCs were previously reported to support the metastasis of cell-line xenografts[21]. It will be important to determine whether human MSCs uniquely provide this function in tumor grafts or whether other stromal cells such as fibroblasts, macrophages or other bone-marrow–derived cells may serve redundant functions.

One of the most promising parallels between the breast cancers in the subjects we studied and their corresponding grafts is their ability to spontaneously metastasize. A previous report detailing the transplantation of breast tumors used a subcutaneous engraftment technique and reported frequent metastasis to lungs in 3 out of a total of 17 lines. The subcutaneous approach also resulted in a lower take rate of primary compared to metastatic tumors[22]. In contrast, our take rate was not substantially different between primary and metastatic specimens, and all but one orthotopic tumor-graft line spontaneously metastasized.

Although metastasis to the lymphatics, lungs and peritoneum commonly occurred, we did not find overt signs of metastasis to either liver or brain, which are also common sites of metastasis in people with breast cancer. Several possibilities may explain this conundrum. First, the development of liver and brain metastasis may be a slower process and may yield only micrometastases at the time of necropsy. Primary tumor resection in mice with longer follow-up time or specific labeling of tumor cells may be required to detect lesions in liver or brain. Second, tumor grafts we derived from our subjects may not have the capacity to metastasize to the liver or brain; none of the individuals in our study developed clinical metastasis in these organs. Although we have not yet performed a thorough characterization of frequencies and sites of metastasis for all of the lines, we were able to detect bone metastasis in one line from an individual known to have bone metastasis. Future work will be geared toward examining more mice from each line for site-specific metastasis.

We surmise that the high metastatic potential of our tumor grafts is related to lack of *in vitro* manipulation, although this hypothesis remains to be tested. Direct implantation of tumors may preserve the ability of cells to interact with supporting cells within the microenvironment; such features may be lost in the *in vitro* setting. Another possibility is that tumor-initiating cells[32] may be better preserved by direct implantation. These cells are thought to be important for initiation of metastases at distant sites[33], and retention of tumor-initiating cells may also contribute to the high metastatic potential of grafts[9]. Our data suggest that the ability of cancer cells to grow as tumor grafts and the ability to grow in tissue culture are not always compatible: several of the tumor graft lines did not grow under standard culture conditions (Y.S.D. and Y.-C.L., unpublished data). It is notable that orthotopic implantation of cells lines derived from many cancers other than breast cancers can result in highly metastatic tumors[34]; these data suggest that breast cancer may be particularly sensitive to the environment.

Our data show that the ability of a tumor from an individual with breast cancer to grow as a graft is a key indicator of shorter survival time. Not only does this suggest a potential functional assay for assessing tumor aggressiveness (albeit one not yet practical for clinical use), but it also reinforces the notion that tumor grafts accurately model the cancers from which they are derived. Expansion of our tumor graft collection is underway, as is the generation of sublines containing lentivirally delivered[35] markers with which to follow intravital tumor growth and metastasis.

METHODS

Methods and any associated references are available in the online version of the paper at http://www.nature.com/naturemedicine/.

Accession codes. Raw data from the gene expression and SNP array experiments are publicly available in the Gene Expression Omnibus under the accession number GSE32532. Gene expression data for the pre-clustered intrinsic gene set, after merging with previously obtained data[25], are listed in **Supplementary Table 4**.

Note: Supplementary information is available on the Nature Medicine website.

ACKNOWLEDGMENTS

We are grateful to the individuals who donated tissue toward this endeavor and the Associated Regional and University Pathologists Research Institute staff for performing the clinical stains. This work was supported by funding from the Department of Defense Breast Cancer Research Program (to A.L.W.; BC075015), the American Association for Cancer Research and Breast Cancer Research Foundation (to A.L.W.; 07–60–26–WELM) and the Huntsman Cancer Foundation. We also used the Huntsman Cancer Institute Tissue Resource and Application Core and Comparative Oncology Core facilities, which is supported in part by P30 CA042014 (to the Huntsman Cancer Institute).

AUTHOR CONTRIBUTIONS

Y.S.D., G.W., Y.-C.L., M.T.W.E., C.M. and I.J.S. performed the experiments. S.S.B., E.N., L.N. and R.L.R. provided tissues. Y.S.D., G.W., P.S.B., R.F., B.A.M., B.E.W. and A.L.W. analyzed the data. A.L.W. wrote the paper, and B.E.W. and P.S.B. edited the paper. A.L.W. supervised the project.

COMPETING FINANCIAL INTERESTS

The authors declare no competing financial interests.

Published online at http://www.nature.com/naturemedicine/.
Reprints and permissions information is available online at http://www.nature.com/reprints/index.html.

1. Hait, W.N. Anticancer drug development: the grand challenges. *Nat. Rev. Drug Discov.* **9**, 253–254 (2010).
2. Ethier, S.P. Human breast cancer cell lines as models of growth regulation and disease progression. *J. Mammary Gland Biol. Neoplasia* **1**, 111–121 (1996).
3. Bos, P.D., Nguyen, D.X. & Massague, J. Modeling metastasis in the mouse. *Curr. Opin. Pharmacol.* **10**, 571–577 (2010).
4. Francia, G., Cruz-Munoz, W., Man, S., Xu, P. & Kerbel, R.S. Mouse models of advanced spontaneous metastasis for experimental therapeutics. *Nat. Rev. Cancer* **11**, 135–141 (2011).
5. Neve, R.M. *et al.* A collection of breast cancer cell lines for the study of functionally distinct cancer subtypes. *Cancer Cell* **10**, 515–527 (2006).
6. Kao, J. *et al.* Molecular profiling of breast cancer cell lines defines relevant tumor models and provides a resource for cancer gene discovery. *PLoS ONE* **4**, e6146 (2009).
7. Clarke, R. The role of preclinical animal models in breast cancer drug development. *Breast Cancer Res.* **11** (suppl. 3), S22 (2009).
8. Voskoglou-Nomikos, T., Pater, J.L. & Seymour, L. Clinical predictive value of the *in vitro* cell line, human xenograft, and mouse allograft preclinical cancer models. *Clin. Cancer Res.* **9**, 4227–4239 (2003).
9. Liu, H. *et al.* Cancer stem cells from human breast tumors are involved in spontaneous metastases in orthotopic mouse models. *Proc. Natl. Acad. Sci. USA* **107**, 18115–18120 (2010).
10. Clarke, M.F. A self-renewal assay for cancer stem cells. *Cancer Chemother. Pharmacol.* **56** (suppl. 1), 64–68 (2005).
11. Press, J.Z. *et al.* Xenografts of primary human gynecological tumors grown under the renal capsule of NOD/SCID mice show genetic stability during serial transplantation and respond to cytotoxic chemotherapy. *Gynecol. Oncol.* **110**, 256–264 (2008).
12. Kim, M.P. *et al.* Generation of orthotopic and heterotopic human pancreatic cancer xenografts in immunodeficient mice. *Nat. Protoc.* **4**, 1670–1680 (2009).
13. Daniel, V.C. *et al.* A primary xenograft model of small-cell lung cancer reveals irreversible changes in gene expression imposed by culture *in vitro*. *Cancer Res.* **69**, 3364–3373 (2009).

14. Ding, L. *et al.* Genome remodelling in a basal-like breast cancer metastasis and xenograft. *Nature* **464**, 999–1005 (2010).
15. Carey, L., Winer, E., Viale, G., Cameron, D. & Gianni, L. Triple-negative breast cancer: disease entity or title of convenience? *Nat. Rev. Clin. Oncol.* **7**, 683–692 (2010).
16. Quintana, E. *et al.* Efficient tumour formation by single human melanoma cells. *Nature* **456**, 593–598 (2008).
17. Agliano, A. *et al.* Human acute leukemia cells injected in NOD/LtSz-scid/IL-2Rγ null mice generate a faster and more efficient disease compared to other NOD/scid-related strains. *Int. J. Cancer* **123**, 2222–2227 (2008).
18. Ito, M. *et al.* NOD/SCID/γ(c)(null) mouse: an excellent recipient mouse model for engraftment of human cells. *Blood* **100**, 3175–3182 (2002).
19. Wagner, K.U. Models of breast cancer: *quo vadis*, animal modeling? *Breast Cancer Res.* **6**, 31–38 (2004).
20. El-Haibi, C.P. & Karnoub, A.E. Mesenchymal stem cells in the pathogenesis and therapy of breast cancer. *J. Mammary Gland Biol. Neoplasia* **15**, 399–409 (2010).
21. Karnoub, A.E. *et al.* Mesenchymal stem cells within tumour stroma promote breast cancer metastasis. *Nature* **449**, 557–563 (2007).
22. Marangoni, E. *et al.* A new model of patient tumor-derived breast cancer xenografts for preclinical assays. *Clin. Cancer Res.* **13**, 3989–3998 (2007).
23. van de Vijver, M.J. *et al.* A gene-expression signature as a predictor of survival in breast cancer. *N. Engl. J. Med.* **347**, 1999–2009 (2002).
24. Paik, S. *et al.* A multigene assay to predict recurrence of tamoxifen-treated, node-negative breast cancer. *N. Engl. J. Med.* **351**, 2817–2826 (2004).
25. Parker, J.S. *et al.* Supervised risk predictor of breast cancer based on intrinsic subtypes. *J. Clin. Oncol.* **27**, 1160–1167 (2009).
26. Perou, C.M. *et al.* Molecular portraits of human breast tumours. *Nature* **406**, 747–752 (2000).
27. Sørlie, T. *et al.* Gene expression patterns of breast carcinomas distinguish tumor subclasses with clinical implications. *Proc. Natl. Acad. Sci. USA* **98**, 10869–10874 (2001).
28. Sorlie, T. *et al.* Repeated observation of breast tumor subtypes in independent gene expression data sets. *Proc. Natl. Acad. Sci. USA* **100**, 8418–8423 (2003).
29. Hu, Z. *et al.* The molecular portraits of breast tumors are conserved across microarray platforms. *BMC Genomics* **7**, 96 (2006).
30. Klopp, A.H., Gupta, A., Spaeth, E., Andreeff, M. & Marini, F. III. Concise review: dissecting a discrepancy in the literature: do mesenchymal stem cells support or suppress tumor growth? *Stem Cells* **29**, 11–19 (2011).
31. Kuperwasser, C. *et al.* Reconstruction of functionally normal and malignant human breast tissues in mice. *Proc. Natl. Acad. Sci. USA* **101**, 4966–4971 (2004).
32. Liu, S. & Wicha, M.S. Targeting breast cancer stem cells. *J. Clin. Oncol.* **28**, 4006–4012 (2010).
33. Li, F., Tiede, B., Massague, J. & Kang, Y. Beyond tumorigenesis: cancer stem cells in metastasis. *Cell Res.* **17**, 3–14 (2007).
34. Hoffman, R.M. Green fluorescent protein to visualize cancer progression and metastasis. *Methods Enzymol.* **302**, 20–31 (1999).
35. Welm, B.E., Dijkgraaf, G.J., Bledau, A.S., Welm, A.L. & Werb, Z. Lentiviral transduction of mammary stem cells for analysis of gene function during development and cancer. *Cell Stem Cell* **2**, 90–102 (2008).

ONLINE METHODS

Tissue acquisition and processing. All tissue samples were collected with informed consent from individuals being treated at the Huntsman Cancer Hospital and the University of Utah under a protocol approved by the University of Utah Institutional Review Board. Samples were collected and de-identified by the Huntsman Cancer Institute Tissue Resource and Application Core facility before being obtained for implantation. All primary tumors were from individuals who had not received chemotherapy before tissue collection, and all except one metastatic effusion were from individuals who had been treated with chemotherapy, hormone therapy and/or radiation therapy (**Supplementary Table 1**).

Tissue implantation. The University of Utah Institutional Animal Care and Use Committee reviewed and approved all mouse experiments. There were always a minimum of three mice per experimental group, and only female mice were used. We implanted a single fragment of fresh or frozen tumor (~8 mm^3), or 1×10^6 cells in Matrigel, into cleared inguinal mammary fat pads of 3–4-week-old female NOD-SCID mice. Interscapular estrogen pellets were also subcutaneously implanted in mice with ER^+ tumors. Tumor growth was measured weekly using calipers. When tumors reached 150–2,000 mm^3, the mice were killed, and tissue fragments were retransplanted into another cohort of mice, frozen for later use and/or analyzed for histology, gene expression and DNA copy number. Tumor volumes were calculated using the formula $\frac{1}{2} \times \text{length} \times (\text{width})^2$. For the experiments we performed to determine estrogen dependence, ER^+ tumors were implanted into mice as described above in the presence or absence of intrascapular estrogen pellets and with or without a concurrent surgical procedure to remove the ovaries, which was performed according to standard methods.

Preservation of viable tumor tissue. Freshly collected tumor tissues from human subjects or mice were cut into ~8-mm^3 pieces and and stored in liquid nitrogen in a solution of 95% FBS and 5% DMSO for later implantation. Alternatively, the tissue was digested with collagenase solution (1 mg ml^{-1} collagenase (type IV; Sigma) in RPMI-1640 supplemented with 2.5% FBS, 10 mM HEPES and 10 μg ml^{-1} penicillin plus streptomycin) at 37 °C for 40–60 min while shaking at 250 r.p.m. Digested tissue was strained to remove debris and washed in human breast epithelial cell medium (DMEM/F12 supplemented with 10 mM HEPES, 5% FBS, 1 mg ml^{-1} BSA, 0.5 μg ml^{-1} hydrocortisone, 50 μg ml^{-1} gentamycin and 1 μg ml^{-1} ITS-X100) three times. The pellet was resuspended in freezing medium (5% FBS and 10% DMSO in human breast epithelial cell medium) and stored in liquid nitrogen.

Mesenchymal stem-cell experiments. Human mesenchymal stem cells from bone marrow aspirates were obtained from Thermo Fisher Scientific and were successfully cultured for approximately eight passages. The cells were cultured in hMSC expansion medium (AdvanceSTEM mesenchymal stem cell basal medium (HyClone) supplemented with 10% AdvancedSTEM stem cell growth supplement (HyClone)). hMSC cells were collected for use between five and eight passages. We mixed 10^6 hMSCs with 0.5×10^6 cancer cells in 20 μl reduced growth factor Matrigel (BD Biosciences) and injected into cleared mammary fat pads. To track hMSCs during tumor growth, some hMSCs were either infected with a lentivirus expressing GFP or labeled with diI before injection. For analysis of blood vessels, 100-μm cryosections were prepared to visualize the diI-labeled hMSCs and lectin-labeled vessels using a spinning disk confocol microscope (Olympus). We prepared 10-μm cryosections to visualize GFP-expressing hMSCs in combination with immunofluorescent staining. For diI labeling, hMSC cells were detached with trypsin and suspended at a density of 1×10^6 cells per ml in serum-free culture medium. We added 5 μl of diI (Invitrogen) and incubated the mixture for 20 min at 37 °C. The labeled cells were washed twice with serum-free culture medium. For lectin perfusion, mice were deeply anesthetized, and the thoracic skin was opened. Fluorescein-labeled *Lycopersicon esculentum* (tomato) lectin (100 μg per mouse; Vector labs) was injected from the cardiac apex into the left ventricle. After 2 min, the mice were killed, and tumors were collected.

Additional methods. Detailed methodology is described in the **Supplementary Methods**.